Human cytomegalovirus-encoded chemokine receptor US28 promotes tumorigenesis

David Maussang*, Dennis Verzijl*, Marijke van Walsum†, Rob Leurs*, Jens Holl‡, Olivier Pleskoff*, Detlef Michel‡, Guus A. M. S. van Dongen†, and Martine J. Smit*§

*Leiden/Amsterdam Center for Drug Research (LACDR), Division of Medicinal Chemistry, Faculty of Sciences, Vrije Universiteit (VU), De Boelelaan 1083, 1081 HV, Amsterdam, The Netherlands; †Department of Otolaryngology/Head and Neck Surgery, VU Medical Center, 1081 HV, Amsterdam, The Netherlands; and ‡Abteilung Virologie, Universitätsklinikum, Albert-Einstein-Allee 11, 89081 Ulm, Germany

Edited by Thomas E. Shenk, Princeton University, Princeton, NJ, and approved July 3, 2006 (received for review May 29, 2006)

Human cytomegalovirus (HCMV) is a widely spread herpesvirus, suggested to play a role in tumor progression. US28, a chemokine receptor encoded by HCMV, binds a broad spectrum of chemokines and constitutively activates various pathways linked to proliferation. Our studies reveal that expression of US28 induces a proangiogenic and transformed phenotype by up-regulating the expression of vascular endothelial growth factor and enhancing cell growth and cell cycle progression. US28-expressing cells promote tumorigenesis when injected into nude mice. The G protein-uncoupled constitutively inactive mutant of US28, induces delayed and attenuated tumor formation, indicating the importance of constitutive receptor activity in the early onset of tumor development. Importantly, also in glioblastoma cells infected with the newly isolated clinical HCMV strain Titan, US28 was shown to be involved in the HCMV-induced angiogenic phenotype. Hence, the constitutively activated chemokine receptor US28 might act as a viral oncogene and enhance and/or promote HCMV-associated tumor progression.

cancer | G protein-coupled receptor | VEGF | viral infection | drug target

Human cytomegalovirus (HCMV) is a widely spread β-herpesvirus that prevails in 30–90% of the population (1). In immunocompetent hosts, the virus remains in a latent form, but in immunocompromised hosts, like organ transplant recipients and individuals with AIDS, HCMV infection can lead to severe pathologies such as pneumonitis, hepatitis, and retinitis (1). Moreover, HCMV has been associated with chronic diseases, including, for example, vascular diseases (2) and malignancies such as colon cancer (3) and malignant glioma (4). Although the causative role for HCMV in the development of malignancies remains to be established, various HCMV proteins and DNA have been detected with high frequency in tumor tissues (3, 4). In addition, it has been shown that HCMV preferentially infects tumor cells because they present a favorable environment for the virus to exert its oncogenic potential (5). HCMV infection up-regulates different growth factors and cytokines resulting in enhanced cell survival, proliferation, and angiogenesis (5). As such, HCMV appears to enhance the malignant behavior of tumor cells, implying an oncomodulatory role for the virus.

HCMV encodes four G protein-coupled receptors, US27, US28, UL33, and UL78, showing highest homology to human chemokine receptors (6). This latter class of receptors plays a fundamental role in the control and regulation of the immune system, but some (e.g., CXCR4) have recently been shown to play a prominent role in cancer and, more specifically, metastasis (7). In fact, the Kaposi's sarcoma-associated herpesvirus-encoded chemokine receptor ORF74 induces angioproliferative lesions that morphologically resemble Kaposi's sarcoma-like lesions when expressed *in vivo* (8). As such, ORF74 is regarded as a causative agent of Kaposi's sarcoma.

The viral chemokine receptor US28 has been by far the most extensively studied of the four HCMV-encoded G protein-coupled receptors (9). It binds a broad spectrum of chemokines, including CCL2/MCP-1, CCL5/RANTES, and CX3CL1/Fraktalkine, and, unlike its cellular homologue CCR1, exhibits constitutive activity (10). US28 has been shown to constitutively activate signaling pathways linked to proliferation and migration when expressed *in vitro* but also after HCMV infection (11, 12). Moreover, US28 shows promiscuous G protein coupling, constitutively signaling, for example, through $G\alpha_q$ proteins, and is able to potentiate signaling of cellular $G\alpha_i$-linked chemokine receptors (10, 13, 14). Hence, HCMV may effectively use US28 to orchestrate multiple signaling networks within infected cells. US28 might be of key importance in subverting cellular signaling and contribute to the onset and/or progression of tumorigenesis.

To assess the oncogenic potential of US28, we performed *in vitro* and *in vivo* experiments with wild-type (WT) and constitutively inactive US28-expressing cells. In addition, we examined the angiogenic status of cells, infected with either the newly isolated clinical HCMV strain Titan or its US28 deletion mutant.

Results

US28 Induces a Transformed Phenotype in NIH-3T3 Cells. To study the role of US28 in cellular transformation, we stably transfected the mouse fibroblast NIH-3T3 cell line with either US28-wild type or the G protein-uncoupled mutant of US28 (US28-$R^{129}A$), which has previously been shown to be devoid of G protein-mediated signaling (15). Different clones of each cell line were generated, and various clones were analyzed (all data shown are representative for different clonal cell lines). Clonal cell lines expressing US28-WT or US28-$R^{129}A$ showed specific binding of ^{125}I-CCL5, whereas constitutive inositol phosphate (InsP) production was only observed for US28-WT, demonstrating proper surface expression and expected signaling properties of both receptors (Fig. 1*A*). The observed increases in CCL5 binding and InsP production were comparable with previously published data on HCMV-infected cells (14), indicating that the expression levels of US28 in NIH-3T3 cells reflected conditions under viral infection. When cells were cultured in regular medium, the US28-WT expressing cells displayed increased growth rate (Fig. 1*B*). Whereas mock transfected and US28-$R^{129}A$ expressing cells stopped growing upon reaching 100% confluency, the growth rate of US28-WT expressing cells was not decreased. These studies were further corroborated by measuring ^{3}H-thymidine incorporation (Fig. 1*C*). DNA synthesis upon serum starvation (0.5% serum-containing medium) was four-fold higher in US28-WT-expressing cells than in mock transfected and US28-$R^{129}A$-expressing cells. To confirm the oncogenic potential of US28, a

Conflict of interest statement: No conflicts declared.

This paper was submitted directly (Track II) to the PNAS office.

Abbreviations: HCMV, human cytomegalovirus; P.I., proliferation index.

§To whom correspondence may be addressed at: Leiden/Amsterdam Center for Drug Research (LACDR), Division of Medicinal Chemistry, Faculty of Sciences, Vrije Universiteit Amsterdam, De Boelelaan 1083, 1081 HV Amsterdam, The Netherlands. E-mail: mj.smit@few.vu.nl.

© 2006 by The National Academy of Sciences of the USA

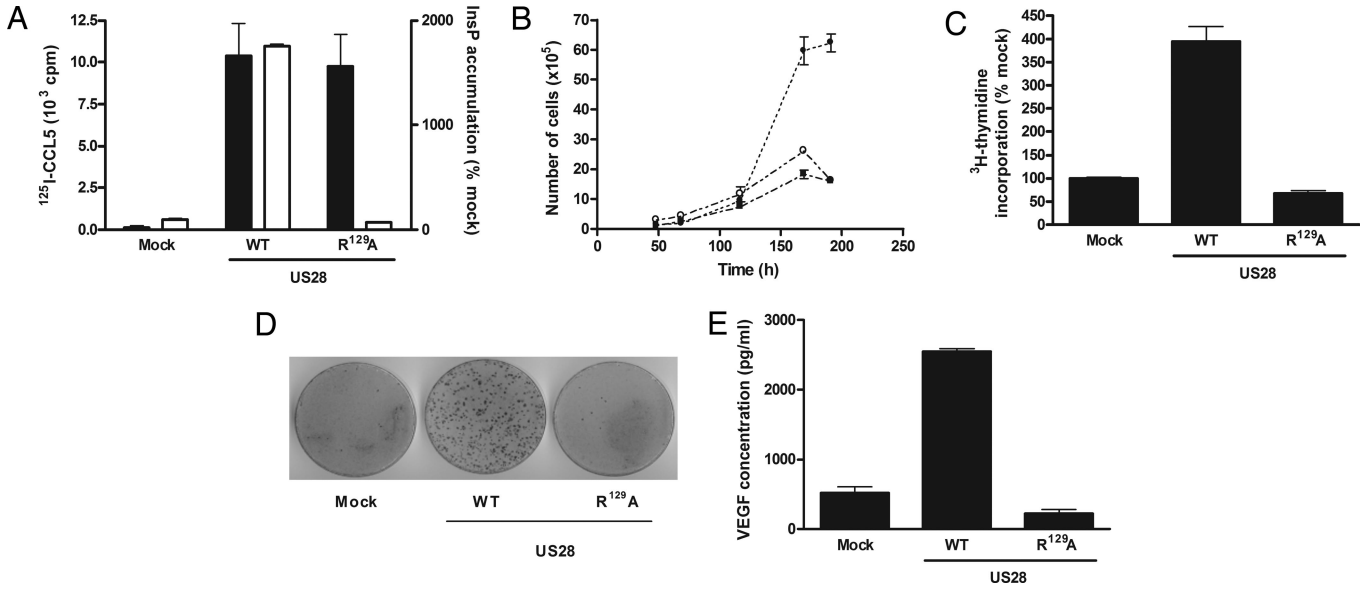

Fig. 1. US28 induces a transformed and proangiogenic phenotype in stably transfected NIH-3T3 cells. (*A*) NIH-3T3 cells were stably transfected with either mock, US28-WT, or US28-R^{129}A (G protein-uncoupled mutant). Both US28 receptors showed specific ^{125}I-CCL5 binding (black bars), determined with Fraktalkine/CX3CL1 10^{-7}M, whereas only the WT receptor constitutively increased the formation of inositol phosphate (InsP). (*B*) Representative cell growth curves of mock-transfected (■), US28-WT- (●), and US28-R^{129}A-(○) expressing cell lines, showing the enhanced growth of US28-WT expressing cells. (*C*) Upon serum starvation, the incorporation of ^{3}H-thymidine was higher in US28-WT-expressing cells compared with mock-transfected and US28-R^{129}A-expressing cells. (*D*) Focus formation assay showing that only US28-WT-expressing cells lost their contact inhibition abilities leading to the formation of numerous foci, whereas the mock and US28-R^{129}A-transfected cells only formed a limited number of foci. (*E*) When cultured for 5 days, NIH-3T3 cells expressing US28-WT produced higher amounts of vascular endothelial growth factor (VEGF) protein compared with mock-transfected and inactive mutant-expressing cells. Data represent mean ± SEM of representative experiments.

focus formation assay was performed, which showed that only US28-WT-expressing cells induced foci formation (Fig. 1*D*). The cell lines expressing the G protein-uncoupled mutant US28-R^{129}A or mock-transfected cell lines showed no foci formation because of the contact inhibition when cells reached confluency. Additionally, we investigated whether US28 also induces an angiogenic phenotype in the stably transfected NIH-3T3 cells by measuring the production of the angiogenic vascular endothelial growth factor (VEGF). After 5 days of culture, the US28-WT expressing cells secreted five-fold more VEGF protein compared with mock-transfected and US28-R^{129}A-expressing cells (respective VEGF concentrations were 521 ± 87 for mock, 2,548 ± 47 for US28-WT cells, and 223 ± 61 pg/ml for US28-R^{129}A cells) (Fig. 1*E*). Thus, the constitutive activation of G proteins by US28 promotes a transformed phenotype in the NIH-3T3 cell line through increased growth rate, enhanced DNA synthesis, and loss-of-contact inhibition, as well as an proangiogenic phenotype mediated by VEGF.

US28 Enhances the Cell Cycle Progression of NIH-3T3 Cells. One of the characteristics of transformed cells is enhanced cell cycle progression. Stably transfected NIH-3T3 cells were assayed to determine the populations of cells present in the different phases of the cell cycle, and the proliferation index (P.I.), defined as the ratio between S, G_2/M cells and G_0/G_1 cells (P.I. = SG_2M/G_0G_1), was calculated. Cells were first synchronized during 24 h by serum starvation (0.5% serum-containing medium) and further stimulated for 24 h by using 10% serum-containing medium. Cell cycle analysis revealed that the US28-WT-expressing cells were more represented in the S and G_2/M phases, whereas the G_1 population was reduced (Fig. 2*A* showing a representative experiment). As a result, the P.I. was on average twice as high for US28-WT-expressing cells when compared with mock-transfected cells (respectively 0.70 ± 0.06 and 0.37 ± 0.03). US28-R^{129}A-expressing cells had a lower P.I. (0.50 ± 0.06) compared with US28-WT-expressing cells. The different P.I. of the three cell lines were significantly different from each other ($P < 0.001$) indicating that the US28 proliferative phenotype is not solely G protein-mediated.

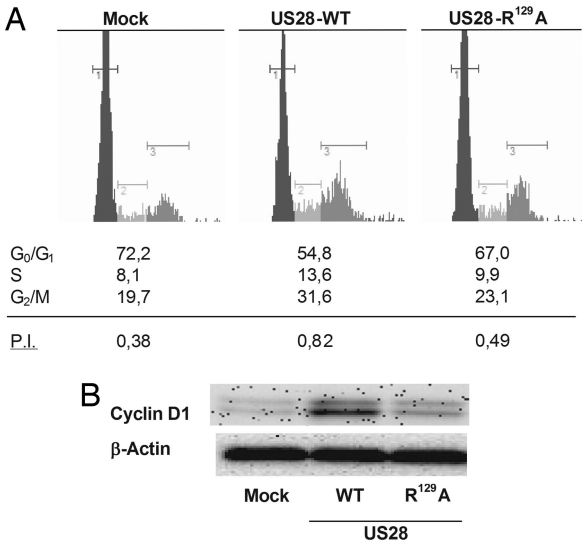

Fig. 2. US28 enhances proliferation through increased cell cycle progression and cyclin D1 expression. (*A*) Stably transfected cells were analyzed with the GUAVA Cell Cycle flow cytometer (Stamford, U.K.). After synchronization of the cells by serum starvation, cells were grown in regular medium, and US28-WT-expressing cells showed an enhanced cell cycle progression compared with mock-transfected cells. US28-R^{129}A expressing cells had an intermediate proliferation index in comparison with US28-WT-expressing and mock-transfected cells. (*B*) Western blot analysis of total cell lysates showed that US28-WT induced the up-regulation of cyclin D1 compared with mock-transfected and US28-R^{129}A-expressing cells. Data are mean ± SEM of representative experiments.

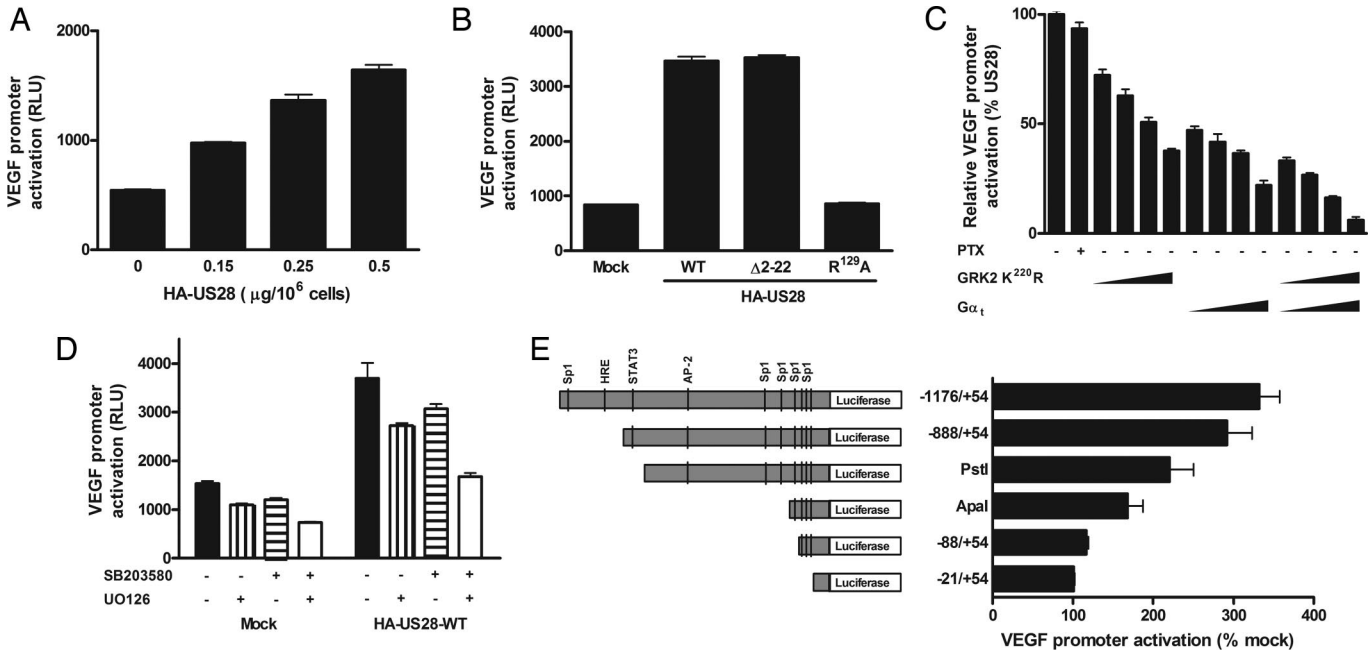

Fig. 3. US28 constitutively activates VEGF promoter. (*A*) In transiently transfected COS-7 cells, HA-US28-WT induced a dose-dependent constitutive activation of the VEGF gene promoter. (*B*) In the VEGF-reporter gene assay, only the N terminus deleted Δ2–22-US28 mutant induced a VEGF promoter activation similar to the WT receptor, whereas the G protein-uncoupled US28-$R^{129}A$ mutant showed no VEGF promoter activation. (*C*) G protein-coupled receptor kinase 2 dominant negative GRK2-$K^{220}R$ and $G\alpha_{transducin}$ ($G\alpha_t$) were cotransfected in different ratios with US28 (scavenger:US28 ratios were 0.5, 1, 2, and 4) into COS-7 cells and showed a dose-dependent VEGF inhibition, involving both $G\alpha_{q/11}$ and $\beta\gamma$ subunits. (*D*) The use of kinases inhibitors UO126 (1 μM) and SB203580 (2 μM) revealed that MAPKs p44/42 and p38, respectively, are independently involved in US28-mediated VEGF gene promoter activation. (*E*) VEGF promoters of different lengths possess different binding sites for transcription factors (AP-2, activator protein-2; Sp1, stimulating protein 1; HRE, hypoxia inducible factor-1 responsive element; STAT3, signal transducer and activator of transcription 3). The US28-mediated VEGF promoter activation was related to the length of the promoters, highlighting the involvement of transcription factors such as the hypoxia inducible factor-1 (HIF-1), STAT3, AP-2, and Sp1.

Increased oncogene-driven cell growth has been attributed to the up-regulation of proteins involved in the different check points of the cell cycle, such as cyclin D1, which mediates the transition from the G_1 phase to the S phase (16). Stably transfected NIH-3T3 cells were synchronized in 0.5% serum-containing medium for 24 h and further stimulated for 24 h with regular culture medium, and total lysates were analyzed by Western blot for cyclin D1 expression (Fig. 2*B* showing a representative figure). US28-WT-expressing cells clearly showed an up-regulation of cyclin D1 protein expression when compared with mock-transfected and US28-$R^{129}A$-expressing cells (relative band intensity: mock, 100 ± 0%; US28-WT, 250 ± 41%; US28-$R^{129}A$, 165 ± 11%). Thus, the constitutive activity and G protein coupling of US28 appear essential for its transforming potential as measured by the enhanced cell cycle progression and up-regulation of cyclin D1 expression.

US28 Constitutive Activity Induces VEGF Gene Expression. As VEGF protein expression was shown to be constitutively up-regulated by US28, we investigated the mechanism by which US28 activated the VEGF promoter. For this purpose, COS-7 cells were transiently transfected with increasing concentrations of $pcDEF_3$ vector containing the hemagglutinin (HA)-tagged US28 WT receptor (HA-US28-WT) cDNA. US28 transfection resulted in a dose-dependent enhancement of cell surface receptor expression, as detected by ^{125}I-CCL5 binding, as well as in a constitutive increase in inositol phosphate (InsP) formation (see Fig. 6*A*, which is shown as supporting information on the PNAS web site). COS-7 cells were also cotransfected with increasing concentrations of HA-US28-WT and a luciferase-based reporter gene containing the VEGF gene promoter spanning region −1176/+54 (VEGF-Luc). As can be seen in Fig. 3*A*, US28 induced a constitutive dose-dependent increase in VEGF promoter activation. The contribution of the constitutive activity of US28 and the involvement of chemokine binding were assessed by using the G protein-uncoupled mutant of US28, HA-US28-$R^{129}A$, which is still able to bind chemokines but is not capable of signaling through G proteins (15), and the N terminus-deleted mutant of US28, HA-Δ2–22-US28, which cannot bind chemokines but can still signal (11) (see Fig. 6*B*). Results showed that the constitutive activation of G proteins by US28, rather than the binding of endogenous chemokines, is crucial for VEGF promoter activation because the VEGF activation was completely abrogated for US28-$R^{129}A$ (Fig. 3*B*). By inducing VEGF promoter activation, US28 might constitutively induce angiogenic processes, essential for an oncogenic phenotype.

US28 Activates VEGF Promoter Via $G\alpha_q$, $G\beta\gamma$, p38, and p44/42 Kinases. Unlike most cellular chemokine receptors that couple to $G\alpha_{i/o}$ proteins, US28 additionally couples to $G\alpha_q$, known to activate proliferative signaling pathways (17). To determine which signaling pathways are activated by US28 leading to VEGF gene expression, we assessed the involvement of $G\alpha_{i/o}$, $G\alpha_q$, and $G\beta\gamma$ proteins, as well as the role of mitogen-activated protein kinases (MAPKs), by using pertussis toxin (PTX) and cotransfection with $G\alpha_q$ and $G\beta\gamma$ scavengers and kinase inhibitors, respectively. Our results indicated that US28-mediated VEGF activation is PTX-insensitive, showing that $G\alpha_{i/o}$ proteins are not involved in US28-mediated VEGF gene expression (Fig. 3*C*). By cotransfecting the dominant negative of G protein-coupled receptor kinase 2 (GRK2) $K^{220}R$ or $G\alpha_{transducin}$ ($G\alpha_t$), known to scavenge both $G\alpha_{q/11}$ and $G\beta\gamma$ or only $G\beta\gamma$, respectively, we clearly observed a dose-dependent inhibition of VEGF activation. When both scavengers were over-expressed together, the inhibition was almost complete, confirming the involvement of both $G\alpha_q$ and $G\beta\gamma$ subunits (Fig. 3*C*). Using specific inhibitors of the

p38 and p44/42 MAPK, respectively, SB203580 and UO126, US28-mediated VEGF promoter activation could be inhibited to a great extent (Fig. 3*D*). When using both inhibitors, both pathways were shown to be independently involved, as measured by enhanced inhibition. To determine the involvement of various transcription factors in the US28-mediated VEGF gene promoter activation, we used different deletion mutants of the VEGF luciferase reporter gene (18). Upon truncation of the VEGF promoter, the US28-mediated luciferase activation decreased to be completely abolished when the promoter reached a minimum length (spanning region −27/+54). As shown in Fig. 3*E*, the hypoxia inducible factor-1 (HIF-1), signal transducer and activator of transcription 3 (STAT3), activator protein-2 (AP-2), and stimulating protein 1 (Sp1) were important transcription factors involved in the US28-induced VEGF promoter activation. Our results indicate that US28 employs $G\beta\gamma$ and $G\alpha_{q/11}$ proteins and the p38 and p44/42 MAPK to activate downstream transcription factors including HIF-1, STAT3, AP-2, and Sp1 to induce VEGF promoter activation.

US28 Promotes Tumor Formation *in Vivo*. Because our *in vitro* studies showed that US28 induced a transformed and proangiogenic phenotype, we determined whether US28-WT expressing cells could also induce tumor formation *in vivo* (Fig. 4*A*). To this end, stably transfected NIH-3T3 cells were s.c. injected in both flanks of nude mice (8 mice injected per cell line; 16 inoculations). First signs of tumor formation appeared as early as 1 week postinjection for the US28-WT group. The presence of tumors was obvious 2 weeks after inoculation. (Fig. 4*B*). All of the US28-WT-injected mice presented tumors at all inoculation sites 3 weeks after injection, after which they were killed. At this time point, both the mock and the US28-R^{129}A groups did not show any tumor formation (Fig. 4*A*). However, 6 weeks postinjection, the US28-R^{129}A group started showing tumors. These tumors grew at a slower rate compared with the US28-WT group, and they did not appear at all inoculated sites (81% take rate for the US28-R^{129}A group) (Fig. 4*B*). The mock group did not develop any tumor, even as long as 75 days after injection. As a control, gene expression of US28 was confirmed by RT-PCR in all of the tumors formed (Fig. 4*C*). These data indicate that the constitutive activation of G proteins by US28 is a key player in the early onset of tumor formation. However, non-G protein signaling pathways might also contribute to the tumorigenic properties of this receptor.

Because the tumors appeared highly vascularized and US28-WT induced the production of VEGF *in vitro*, we investigated the VEGF plasma levels in the three different groups. Three weeks after inoculation, the VEGF plasma levels in the mock, US28-WT, and US28-R^{129}A groups were, respectively, 61 ± 18, 140 ± 40, and 83 ± 23 pg/ml, showing that US28-WT constitutive activity had led to an increase in the VEGF plasma level, which might explain the earlier and stronger onset of tumorigenesis. In addition, tumors of both US28-WT and US28-R^{129}A groups stained positive for the presence of VEGF (Fig. 4*D Upper*), showing that VEGF might have a direct role on the site of the tumor, most likely by inducing angiogenesis. To check for the presence of newly formed blood vessels, immunostaining against CD31 was performed. As shown in Fig. 4*D Lower*, all tumors (US28-WT and US28-R^{129}A) stained positive for CD31, confirming the angiogenic processes in the tumors induced by both receptors, WT and mutant. The *in vivo* experiment clearly demonstrated the tumorigenic properties of US28 that were accompanied by VEGF secretion and formation of new blood vessels within the tumor.

US28 Is Responsible for HCMV-Induced Angiogenic Phenotype. To determine the importance of US28 in the viral context, we evaluated the impact of the deletion of the US28 gene in a newly

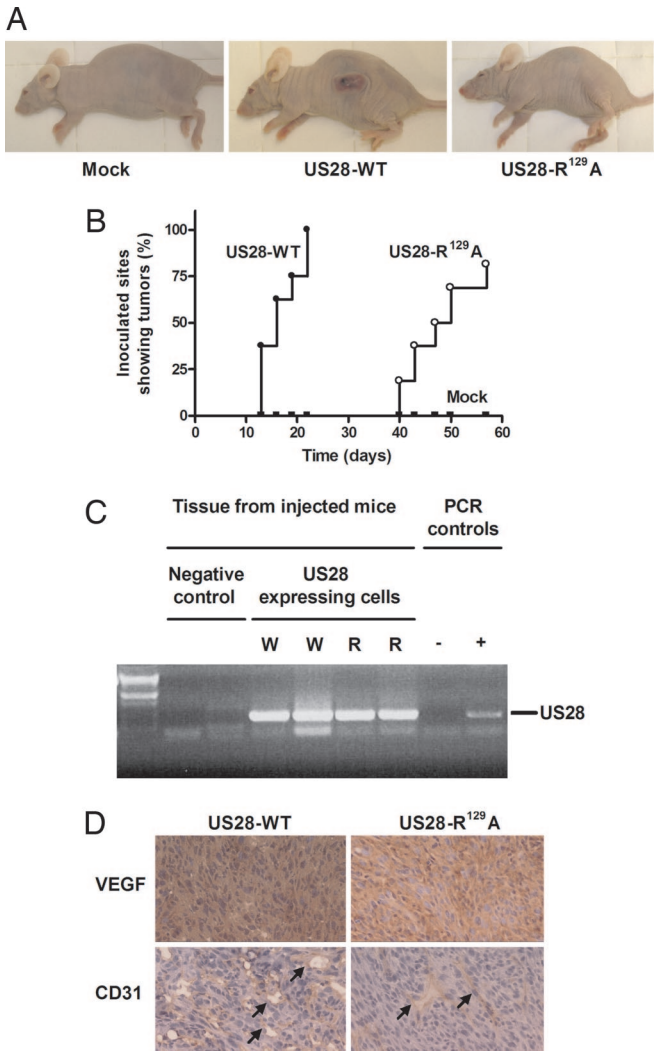

Fig. 4. US28 promotes tumor formation *in vivo*. (*A*) Nude mice were injected with mock, US28-WT-, and US28-R^{129}A-expressing NIH-3T3 cells. Three weeks after inoculation of the cells, the US28-WT group was the only group showing extensive tumor formation. (*B*) Kaplan–Meier curves presenting inoculation sites showing tumor formation in the $pcDEF_3$ (■), US28-WT (●), and US28-R^{129}A (○) groups (8 mice and 16 inoculation sites). The US28-R^{129}A group showed delayed tumor formation compared with the US28-WT, and also a lower take rate (81% versus 100%). The mock group showed no tumor formation during the 75 days observation period. (*C*) PCR showing the presence of US28 DNA in mice injected with NIH-3T3 cells expressing US28-WT (W) and US28-R^{129}A (R). (*D*) VEGF presence (red) (*Upper*) and the formation of new blood vessels (indicated by the arrow) with CD31 staining (red) (*Lower*) in the formed tumors.

established clinical HCMV strain (Titan). The virus was isolated from an infected patient according to the technique of Borst *et al.* (19). The US28 deletion mutant of HCMV (HCMV-ΔUS28) showed neither US28 transcription or binding of CCL5 (see Fig. 7, which is published as supporting information on the PNAS web site). Because HCMV has been shown to induce the production of VEGF (20) and it has been linked to the development of glioma (4), we studied the effect of HCMV-WT and HCMV-ΔUS28 on VEGF regulation in the HCMV-permissive glioblastoma cell line U373. Infection of U373 cells showed that HCMV-WT strongly activated the VEGF promoter (Fig. 5). This activation was severely attenuated with the deletion mutant HCMV-ΔUS28, and it was not significantly different from the activation in mock-infected cells ($P > 0.05$). These data indicate

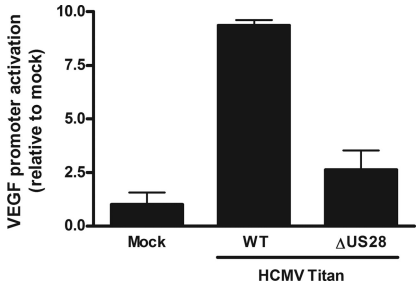

Fig. 5. US28 is involved in HCMV-induced VEGF up-regulation. U373 cells infected with HCMV (HCMV-WT) and the HCMV deletion mutant of US28 (HCMV-ΔUS28) showed that US28 plays a major role in the VEGF gene promoter activation in infected cells.

that US28 plays a crucial role in the VEGF promoter activation in HCMV-infected cells.

Discussion

It is well established that some DNA viruses induce oncogenesis. Human papilloma virus (HPV) and Kaposi's sarcoma-associated herpesvirus (KSHV), for example, are the etiological agent of, respectively, cervical cancer (21) and Kaposi's sarcoma (22), and Epstein–Barr virus (EBV) is associated with Burkitt's lymphoma and Hodgkin's disease (23). Unlike these oncogenic viruses, HCMV infection fails to transform susceptible normal cells. Yet, in tumor cells, as observed for oncoproteins of HPV types 16 and 18, and human adenovirus, some HCMV-encoded proteins possess oncomodulatory properties, modulating key signaling pathways, thereby promoting tumor cell proliferation (5). Interestingly, HCMV, like Kaposi's sarcoma-associated herpesvirus, encodes a viral chemokine receptor, that, unlike its cellular homologue, binds a broad spectrum of chemokines and displays constitutive activity (9). The Kaposi's sarcoma-associated herpesvirus-encoded receptor ORF74 has previously been shown to act as a viral oncogene, inducing angioproliferative lesions that morphologically resemble Kaposi's sarcoma (8). In this study, we demonstrate that the HCMV-encoded chemokine receptor US28 might act as a viral oncogene. Expression of US28 in NIH-3T3 cells induces transformation and promotes tumorigenesis *in vivo*, in part by activating proangiogenic signaling pathways. In nontumorigenic cells, however, we have recently shown that US28 induces apoptosis (24), indicating that the oncomodulatory properties of US28 are only apparent when cells present a tumorigenic phenotype or are on the verge of transformation, such as NIH-3T3 cells. A hallmark of the viral-encoded chemokine receptors is their ability to signal in a constitutively active manner (9). This property appears essential in the early onset of tumorigenesis induced by US28, as shown by the delayed and attenuated tumor formation by the US28-$R^{129}A$ mutant. Although the mutation in the DRY motif of US28-$R^{129}A$ prevents G protein activation, some residual activity such as a slightly enhanced proliferation index and increased expression of cyclin D1 might account for the tumor formation in mice injected with US28-$R^{129}A$-expressing cells. As shown for other receptors (25), US28 might also use G protein-independent signaling pathways to exert its oncogenic potential. In particular, because the US28-$R^{129}A$ mutant is not devoid of chemokine binding, chemokines may activate US28, stimulating non-G protein signaling pathways.

Also in infected U373 cells, HCMV induced VEGF promoter activation. When using the newly developed clinical HCMV US28 deletion strain, this VEGF promoter activation was not apparent, indicating that US28 is essential for the angiogenic phenotype observed after viral infection. As such, after HCMV infection, US28 might act in a concerted manner with other HCMV-encoded proteins, which were previously linked to oncogenesis, such as the viral homologue of interleukin-10 (cmvIL-10) (26, 27) and immediate-early proteins (28). The constitutive activity of US28 and its ability to bind chemokines, known to be markedly expressed in certain types of cancer (7), might facilitate progression of tumor formation after infection. In particular, reactivation of HCMV in immunocompromised cancer patients might boost expression of US28, further promoting the oncogenic potential of HCMV. In view of its tumorigenic properties, US28 can be regarded as a potential drug target for the treatment of HCMV-related proliferative diseases.

Materials and Methods

Cell Culture. African green monkey COS-7 cells, human glioblastoma U373 cells, and mouse fibroblast NIH-3T3 cells were cultured in DMEM supplemented with 10% of fetal calf, heat inactivated fetal calf, and calf sera, respectively. Transfections were performed in COS-7 by using the diethyl-amino-ethyl-dextran method (10) and in U373 and NIH-3T3 cells by using the calcium phosphate method. Stably transfected NIH-3T3 cells were selected and maintained in culture with neomycin (400 μg/ml) to ensure homogenous expression of US28 receptors.

US28 Receptor Characterization and Thymidine Incorporation. US28 expression and constitutive signaling were checked by using ^{125}I-CCL5 binding (specific binding was measured by using Fraktalkine/CX3CL1 10^{-7}M) and ^{3}H-inositol phosphate formation as described (10). As for thymidine incorporation measurement, the experiment was carried out upon serum starvation by using medium containing 0.5% calf serum (29).

Reporter Gene Analysis. The VEGF reporter gene plasmids were composed of different lengths of the VEGF promoter, hence containing different binding sites for transcription factors as described (18). For the VEGF promoter activation measurements, 10^6 COS-7 cells were transfected with 5 μg of pGL2-VEGF-Luciferase plasmid and the indicated amounts (or 0.5 μg when not stated) of pcDEF$_3$-HA-US28 receptors (wild type, G protein-uncoupled mutant $R^{129}A$, and N terminus deleted Δ2–22). When using inhibitors or G protein scavengers, they were respectively added or cotransfected together with US28 (total DNA amounts were kept constant using empty vector). In U373 infected cells, transfection of the VEGF-Luciferase plasmid (30) was performed 2 h post infection (multiplicity of infection 1). Luciferase activities were measured 24 h after transfection.

Focus Formation Assay. The focus formation assay was performed as described by Burger *et al.* (31). Stably transfected NIH-3T3 cells (2×10^3) were cultured with 2×10^5 untransfected NIH-3T3 cells for 2 weeks in regular culture medium without G418.

VEGF ELISA. VEGF amounts released by stably transfected NIH-3T3 cells after 5 days of culture or VEGF present in the plasma of the mice from the *in vivo* study were measured by using a mouse-VEGF Quantikine kit (R & D Systems, Abingdon, U.K.), following the manufacturer's recommended procedures.

Tumor Formation *in Vivo*. All animal experiments were performed according to the National Institutes of Health principles of laboratory animal care and Dutch national law ["Wet op de Dierproeven" (Stb 1985, 336)] and approved by the Dierexperimentencommissie from the VU Medical Center and performed in compliance with the protocol FaCh 05-02. Stably transfected NIH-3T3 cells (2×10^6) containing pcDEF$_3$, pcDEF$_3$-US28-WT, or pcDEF$_3$-US28-$R^{129}A$ plasmids were injected s.c. into the flank of 8- to 10-week-old female nude mice (Hsd, athymic

nu/nu, 25–32 g, Harlan Laboratories/Cambridge Research Biochemicals; Zeist, The Netherlands).

Immunohistochemistry. Cryosections of the US28-WT and US28-$R^{129}A$ tumors were stained for the presence of VEGF and CD31 by using the following antibodies: goat anti-mouse VEGF antibody (AF-493-NA; R & D Systems) (10 μg/ml) with a rabbit-anti-goat-HRP (P 0449; DakoCytomaton, Heverlee, Belgium) (1:100), and rat-anti-mouse CD31 (550274, BD PharMingen Erembodegem, Alphen aan den Rijn, The Netherlands) (1:10) with a mouse-anti-rat-HRP (80–9520, Zymed Laboratories, Breda, The Netherlands) (1:100). Nuclear staining was performed with haematoxylin (Merck, Amsterdam, The Netherlands).

RT-PCR for US28. In the tumors formed, US28 gene expression was checked using standard reverse transcriptase PCR (RT-PCR). The primers used were US28 forward 5′-AGCGTGCCGTGTACGTTAC-3′ and US28 reverse 5′-ATAAAGACAAGCACGACC-3′.

Cell Cycle Analysis. Stably transfected NIH-3T3 cells were synchronized for 24 h in DMEM containing 0.5% calf serum and stimulated using 10% calf serum-containing DMEM for another 24 h. Cells were stained with propidium iodine, and cell cycle populations were determined by using the Guava EasyCyt system according to the manufacturer's recommendations (Guava). The Guava Cell Cycle software was used to determine the cell populations in the different cell cycle phases and the P.I. was quantified from the SG_2M/G_0G_1 ratios.

Western Blot Analysis. Quantification of the cyclin D1 expression levels were performed by Western blot on total cell lysates by using a monoclonal mouse cyclin D1 antibody (05–815; Upstate Biotechnology, Lake Placid, NY) (1 μg/ml). Protein expression levels were related to β-actin expression (A5441; Sigma, St. Louis, MO) (1:10,000).

Cytomegalovirus Strains Creation. The Titan strain was generated from a low passaged clinical isolate by the BAC-technique of Borst *et al.* (19), and the US28-deletion mutant was created by the ET-recombinant method according to Wagner and Koszniwski (32). The HCMV-WT and ΔUS28 strains were characterized by Northern blot and ^{125}I-CCL5 binding as described (14).

Statistical Analysis. All *in vitro* experiments were performed at least three times in triplicates. When different groups or cell lines were compared, one-way ANOVA analysis were performed by using a Tukey posttest with the GraphPad Prism software (San Diego, CA). Bars and error bars on the graphs as well as data in the text represent the mean ± SEM.

We thank Dr. G. Pages (Institute of Signalling Development Biology and Cancer, Nice, France) for providing the different VEGF reporter gene plasmids. This work was supported by The Netherlands Organization for Scientific Research (to D. Maussang and M.J.S.), The Netherlands Technology Foundation (to D.V.), The Royal Netherlands Academy of Arts and Sciences (to M.J.S.), and the Sonderforschungsbereich 451, project A3 (to J.H.).

1. Gandhi, M. K. & Khanna, R. (2004) *Lancet Infect. Dis.* **4,** 725–738.
2. Stassen, F. R., Vega-Cordova, X., Vliegen, I. & Bruggeman, C. A. (2006) *J. Clin. Virol.* **35,** 349–353.
3. Harkins, L., Volk, A. L., Samanta, M., Mikolaenko, I., Britt, W. J., Bland, K. I. & Cobbs, C. S. (2002) *Lancet* **360,** 1557–1563.
4. Cobbs, C. S., Harkins, L., Samanta, M., Gillespie, G. Y., Bharara, S., King, P. H., Nabors, L. B., Cobbs, C. G. & Britt, W. J. (2002) *Cancer Res.* **62,** 3347–3350.
5. Cinatl, J., Jr., Vogel, J. U., Kotchetkov, R. & Wilhelm Doerr, H. (2004) *FEMS Microbiol. Rev.* **28,** 59–77.
6. Chee, M. S., Satchwell, S. C., Preddie, E., Weston, K. M. & Barrell, B. G. (1990) *Nature* **344,** 774–777.
7. Balkwill, F. (2004) *Nat. Rev. Cancer* **4,** 540–550.
8. Yang, T. Y., Chen, S. C., Leach, M. W., Manfra, D., Homey, B., Wiekowski, M., Sullivan, L., Jenh, C. H., Narula, S. K., Chensue, S. W., *et al.* (2000) *J. Exp. Med.* **191,** 445–454.
9. Vischer, H. F., Leurs, R. & Smit, M. J. (2006) *Trends Pharmacol. Sci.* **27,** 56–63.
10. Casarosa, P., Bakker, R. A., Verzijl, D., Navis, M., Timmerman, H., Leurs, R. & Smit, M. J. (2001) *J. Biol. Chem.* **276,** 1133–1137.
11. Casarosa, P., Menge, W. M., Minisini, R., Otto, C., van Heteren, J., Jongejan, A., Timmerman, H., Moepps, B., Kirchhoff, F., Mertens, T., *et al.* (2003) *J. Biol. Chem.* **278,** 5172–5178.
12. Streblow, D. N., Soderberg-Naucler, C., Vieira, J., Smith, P., Wakabayashi, E., Ruchti, F., Mattison, K., Altschuler, Y. & Nelson, J. A. (1999) *Cell* **99,** 511–520.
13. Bakker, R. A., Casarosa, P., Timmerman, H., Smit, M. J. & Leurs, R. (2004) *J. Biol. Chem.* **279,** 5152–5161.
14. Minisini, R., Tulone, C., Luske, A., Michel, D., Mertens, T., Gierschik, P. & Moepps, B. (2003) *J. Virol.* **77,** 4489–4501.
15. Waldhoer, M., Casarosa, P., Rosenkilde, M. M., Smit, M. J., Leurs, R., Whistler, J. L. & Schwartz, T. W. (2003) *J. Biol. Chem.* **278,** 19473–19482.
16. Sherr, C. J. (1996) *Science* **274,** 1672–1677.
17. Radhika, V. & Dhanasekaran, N. (2001) *Oncogene* **20,** 1607–1614.
18. Legros, L., Bourcier, C., Jacquel, A., Mahon, F. X., Cassuto, J. P., Auberger, P. & Pages, G. (2004) *Blood* **104,** 495–501.
19. Borst, E. M., Hahn, G., Koszinowski, U. H. & Messerle, M. (1999) *J. Virol.* **73,** 8320–8329.
20. Reinhardt, B., Schaarschmidt, P., Bossert, A., Luske, A., Finkenzeller, G., Mertens, T. & Michel, D. (2005) *J. Gen. Virol.* **86,** 23–30.
21. Munoz, N., Bosch, F. X., de Sanjose, S., Herrero, R., Castellsague, X., Shah, K. V., Snijders, P. J. & Meijer, C. J. (2003) *N. Engl. J. Med.* **348,** 518–527.
22. Ganem, D. (1997) *Cell* **91,** 157–160.
23. Young, L. S. & Rickinson, A. B. (2004) *Nat. Rev. Cancer* **4,** 757–768.
24. Pleskoff, O., Casarosa, P., Verneuil, L., Ainoun, F., Beisser, P., Smit, M., Leurs, R., Schneider, P., Michelson, S. & Ameisen, J. C. (2005) *FEBS J.* **272,** 4163–4177.
25. Rajagopal, K., Lefkowitz, R. J. & Rockman, H. A. (2005) *J. Clin. Invest.* **115,** 2971–2974.
26. Kotenko, S. V., Saccani, S., Izotova, L. S., Mirochnitchenko, O. V. & Pestka, S. (2000) *Proc. Natl. Acad. Sci. USA* **97,** 1695–1700.
27. Doniger, J., Muralidhar, S. & Rosenthal, L. J. (1999) *Clin. Microbiol. Rev.* **12,** 367–382.
28. Castillo, J. P. & Kowalik, T. F. (2002) *Gene* **290,** 19–34.
29. Westphal, R. S. & Sanders-Bush, E. (1996) *Mol. Pharmacol.* **49,** 474–480.
30. Finkenzeller, G., Sparacio, A., Technau, A., Marme, D. & Siemeister, G. (1997) *Oncogene* **15,** 669–676.
31. Burger, M., Burger, J. A., Hoch, R. C., Oades, Z., Takamori, H. & Schraufstatter, I. U. (1999) *J. Immunol.* **163,** 2017–2022.
32. Wagner, M. & Koszinowski, U. H. (2004) *Methods Mol. Biol.* **256,** 257–268.